Reference: *Biol. Bull.* **192:** 321–331. (April, 1997)

The Route of Ion and Water Movements Across the Gill Epithelium of the Freshwater Shrimp *Macrobrachium olfersii* (Decapoda, Palaemonidae): Evidence From Ultrastructural Changes Induced by Acclimation to Saline Media

JOHN C. McNAMARA[1] AND ALICE GONÇALVES LIMA[2]

[1]*Departamento de Biologia, FFCLRP, Universidade de São Paulo, Ribeirão Preto 14040-901 SP, Brasil; and* [2]*Departamento de Fisiologia, Instituto de Biociências, Universidade de São Paulo, São Paulo, Brasil*

Abstract. The ultrastructure of the pillar cells in the gill lamellae of the freshwater shrimp *Macrobrachium olfersii* was examined to evaluate the routes of salt and water movement across the gill epithelium and into the hemolymph. Alterations were morphometrically quantified in shrimp maintained in fresh water (FW, <0.5‰ salinity) and after acclimation to saline media (21‰ or 28‰ salinity). The tissue interface between the hemolymph and the external medium consists exclusively of the thin apical flange regions of the pillar cells, the upper membrane of which is highly amplified by dense microvilli and overlain by a thin cuticle. The lower flange membrane, bathed by the hemolymph, is smooth and not invaginated. Contiguous flanges are strongly bound by junctional structures including desmosomes and septate junctions. The basal surface of the pillar cell perikaryon is linked to the adjacent septal cells through many basolateral junctions. The septal cell plasmalemma is abundantly and deeply invaginated, each infolding enclosing numerous mitochondria; these characteristics are typical of salt-transporting machinery. After shrimps were acclimated to saline media for 10 days, the thickness of the pillar cell flanges was significantly reduced (from 1.3 to $\approx$0.4 μm), as was the height (from 0.8 to 0.3 μm) and density (from 4.0 to $\approx$ 1.8 microvilli/μm) of the apical microvilli. This reduction in the apical surface area of the pillar cells appears to lead to decreased ionic permeability, concomitant with a reduction in Na^+/K^+-ATPase activity, thus limiting Na^+ uptake. In contrast to the brachyurans, in which the respiratory and ion-transporting mechanisms are differentially located in the anterior and posterior gills, in palaemonid shrimps the pillar cells apparently play a dual role: ions move preferentially through ion transporters in the microvilli above the pillar cell perikaryon, while respiratory gases are exchanged through the fine flange regions in contact with the hemolymph.

Received 6 May 1996; accepted 20 December 1996.

Introduction

Salt uptake in hyperosmoregulating, freshwater decapods and in hyper-regulating, euryhaline brachyurans experimentally exposed to dilute media takes place primarily through the gill tissues (see Mantel and Farmer, 1983; Gilles and Péqueux, 1986; Freire and McNamara, 1995, for discussion and references).

In brachyurans, specific ion-transporting regions of the posterior gills account for much of this salt uptake, while the anterior gills appear to be responsible mainly for respiratory gas exchange (Péqueux, 1995). Such salt-transporting gills exhibit a typical microanatomy: the highly flattened, cuticle-bounded gill lamellae essentially consist of a continuous layer of epithelial cells enclosing a narrow hemolymph space; linked pairs of sustaining pillar cells extend across this space between the opposing epithelial sheets, their apical flanges often forming part of the epithelium (Mantel and Farmer, 1983; Taylor and

Taylor, 1986; Maina, 1990). The apical surfaces of the epithelial cells are characteristically amplified by membrane infoldings in the form of leaflets, whereas the basolateral membranes are deeply invaginated and associated with mitochondria (Copeland, 1968; Copeland and Fitzjarrell, 1968; Gilles and Péqueux, 1985; Maina, 1990). A fenestrated, partial intralamellar septum, which bisects the gill lamella into two symmetrical portions, may be present (Barra *et al.*, 1983; see Taylor and Taylor, 1992, for review).

The apical infolding system of the gill epithelial cells of decapod crustaceans undergoes structural reorganization in response to short-term exposure or acclimation to salinities different from that predominant in the habitat (Bubel, 1976; Compère *et al.*, 1989; see Taylor and Taylor, 1992; Freire and McNamara, 1995, for review and references). After exposure to dilute media, the apical leaflets and microvilli become more numerous and elaborate, and an extracellular, subcuticular compartment enlarges due to osmotic swelling (Gilles and Péqueux, 1985). During short- and medium-term exposure (hours to days) to concentrated media, the apical infolding system is disrupted and regresses while the subcuticular space disappears (see Shires *et al.*, 1994; Péqueux, 1995). The apical region of the epithelial cells thus appears to represent a labile, primary barrier to osmotic alteration deeper within the gill tissue.

The routes by which salt uptake is effected in the gills of hyperosmoregulating, freshwater palaemonid shrimps have received very little attention. Although phyllobranchiate palaemonid gill is comparable to the brachyuran gill in gross morphology, very little is known about its fine structure (*cf.*, Nakao, 1974; Doughtie and Rao, 1978; see Taylor and Taylor, 1992); ultrastructural studies of the effects of acclimation to saline media on the apical infolding system are entirely lacking. Freire and McNamara (1995) analyzed the gill structure of *Macrobrachium olfersii*, a representative freshwater palaemonid shrimp. Each flattened hemilamella constitutes a narrow hemolymph-filled space delimited by the flanges of two opposing layers of pillar cells, the bases of which adjoin in the mid-region of the lamella. A layer of septal cells, contiguous with the pillar cell bases, divides the intralamellar space into two parallel compartments, forming a lattice-like series of lacunae through which the hemolymph flows. The epithelium forming the hemolymph-water interface consists exclusively of the expanded apical flanges of the pillar cell perikarya. The upper membranes of these flange cells are modified to form an extensive system of microvilli, although the lower flange surfaces and perikarya show no membrane-amplifying features that would suggest salt transport. This role has been assumed by the cells of the intralamellar septum, the plasma membranes of which are extensively invaginated and rich in associated mitochondria. Other cell types are rare within the septum.

This relocation of the salt-transporting machinery—from the basolateral membranes of epithelial cells whose apical surfaces are in direct contact with the cuticle adjacent to the external medium, in the brachyurans, to the intralamellar septum, surrounded on both surfaces by flowing, Na^+-rich hemolymph, in the freshwater palaemonids—poses several engaging questions in terms of the physical routes by which salt might be transported across the gill tissue to the hemolymph. The present study thus examines the ultrastructure of the pillar cells, particularly their apical microvilli and junctions, in the gills of *Macrobrachium olfersii*, a strongly hyperosmoregulating, freshwater palaemonid shrimp (McNamara, 1987). Gills were examined both in animals maintained in fresh water (<0.5‰ salinity) and in those acclimated to media considered to be strongly saline (21‰ and 28‰ salinity) for this species.

Materials and Methods

Adult female specimens of *Macrobrachium olfersii*, measuring 4 to 6 cm in total length, were collected some 2 km from the mouth of the Paúba Stream on the southern coast of São Paulo State, Brazil. In the laboratory, the shrimps were maintained in 250-l aquaria in water from the collection site (fresh water [FW], <0.5‰ salinity) and were fed 3 times a week with fish, beef, and carrot.

To examine the effects of exposure to saline media on gill ultrastructure, groups of shrimps in stage $C\text{-}D_0$ of the molt cycle were acclimated to salinities of <0.5‰, 21‰, or 28‰ (20, 630, and 840 mOsm/kg H_2O; 5, 287, and 383 mEq Na^+/l; 5, 335, and 447 mEq Cl^-/l, respectively) over a 10-day period. Salinities, verified using an optical refractometer, were prepared by diluting seawater with FW from the collection site.

After the acclimation period, the ventral nerve cord was severed, the eyestalks and rostrum were removed, and the shrimps were perfused through the ventral abdominal sinus with primary fixative at the rate of 1 ml/min for 10 min. The sixth gill was then dissected, the middle third was removed and bisected, and the two portions, each comprising about 15 lamellae, were placed in primary fixative on ice for 2 h.

The primary fixatives for the different groups of acclimated shrimps were adjusted according to the hemolymph osmolality measured for each group. For shrimps maintained in FW, the fixative consisted of (in millimoles) paraformaldehyde (200), glutaraldehyde (250), sodium cacodylate (100); and Na^+ (28), K^+ (8), Ca^{++} (25), and Mg^{++} (4) as chlorides (effective osmolality 360 mOsm/kg H_2O, pH 7.3). The effective osmolalities (565 and 725 mOsm/kg H_2O) of the fixatives for shrimps

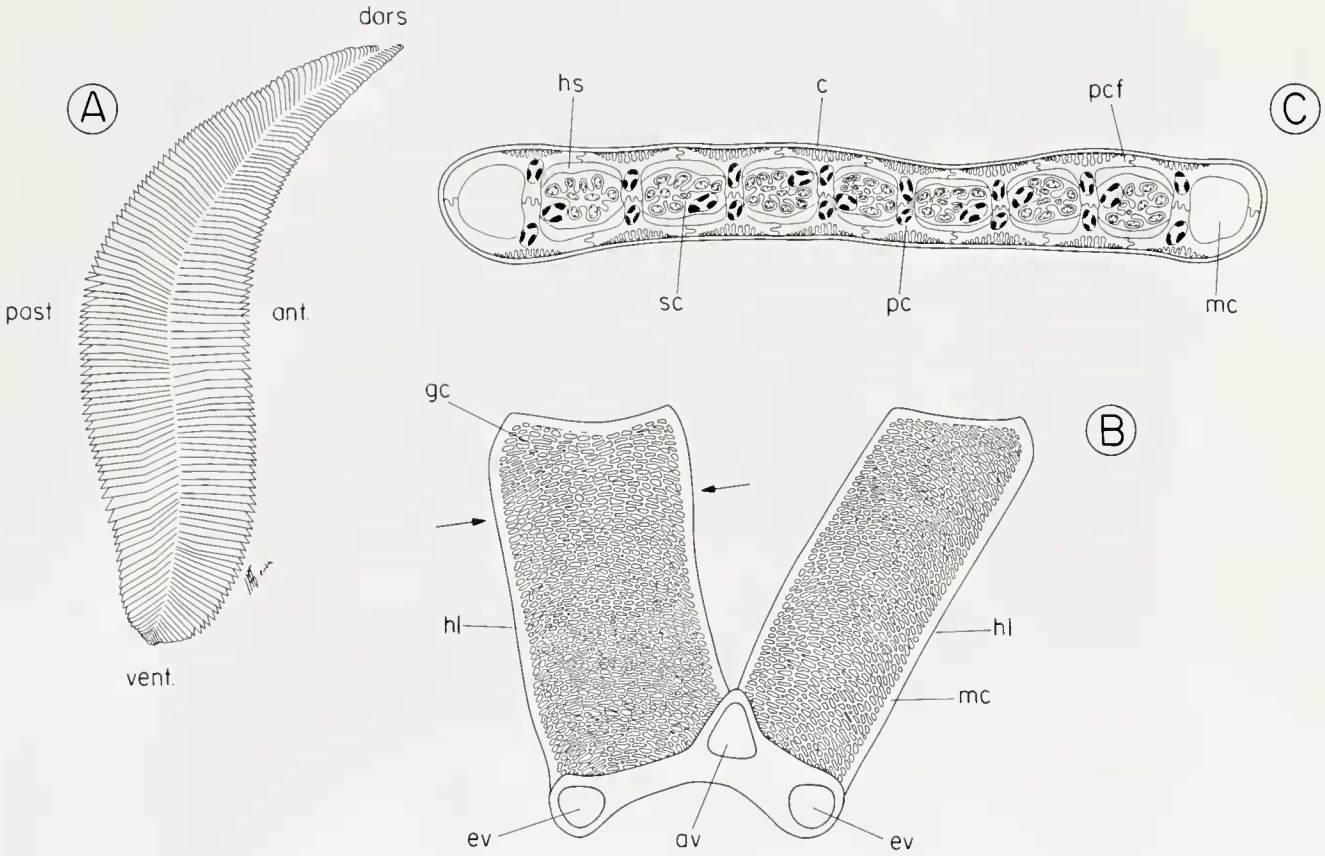

Figure 1. A summary and location diagram showing the general anatomy of the sixth, right posterior gill (A) and of a constituent gill lamella (B) in the freshwater shrimp *Macrobrachium olfersii*. Hemolymph flows from the lateral efferent vessels (ev), through the outer marginal canals (mc), across the hemilamella (hl) by way of the gill capillaries (gc) to the inner marginal canals, and back through the central afferent vessel (av). (C) A cross section of the hemilamella (between arrows in B) reveals the lattice-like organization of the gill tissue, resulting from the semi-regular arrangement of opposing pillar cells (pc). The perikarya of the pillar cells are surrounded by hemolymph spaces (hs) and abut the lateral regions of the median, intralamellar, septal cells (sc). The fine pillar cell flanges (pcf), in contact with the thin cuticle (c), form the primary epithelial interface between the hemolymph and the external medium.

acclimated to saline media of 21‰ and 28‰ were adjusted by using final NaCl concentrations of 140 and 225 m*M*, respectively.

The gill fragments were then rinsed (3 × 5 min) in the respective buffer solutions alone on ice (composition as above, less the aldehydes) and post-fixed in 1% osmium tetroxide in the same buffer systems for 1.5 h on ice.

The fragments were dehydrated in a graded ethanol series (65 min total), transferred into propylene oxide (2 × 15 min), infiltrated overnight, and embedded in Araldite 6005 resin. Thick sections were cut with glass knives at 0.5 μm thickness on a Porter-Blum Sorvall MT2 ultramicrotome, stained with 1% methylene blue and 1% azur II in 1% aqueous borax, and photographed using Kodak T-Max 100 ASA film on a Nikon AFX II photomicroscope. Thin sections of 50–80 nm thickness prepared similarly were stained with aqueous uranyl acetate and Reynolds' (1963) lead citrate and examined at an accelerating voltage of 80 kV in a Jeol 100-CX electron microscope.

The effects of acclimation to the experimental media (<0.5‰, 21‰, or 28‰) were evaluated morphometrically using as criteria the alterations induced in the thickness (in micrometers) of the intralamellar septal cells and the pillar cell flanges; and the height (in micrometers) and numerical density (as microvilli/micrometer of apical membrane) of the apical microvilli on the pillar cells. Measurements were made on between 10 and 15 micrographs of sections taken at random in a plane transverse to the long axis of the gill lamellae (see Fig. 1, and Freire and McNamara, 1995) from 3 to 5 shrimp for each saline medium. The material was photographed at 8000 to 10,000× and the negatives were printed at a final magnification of 25,000×.

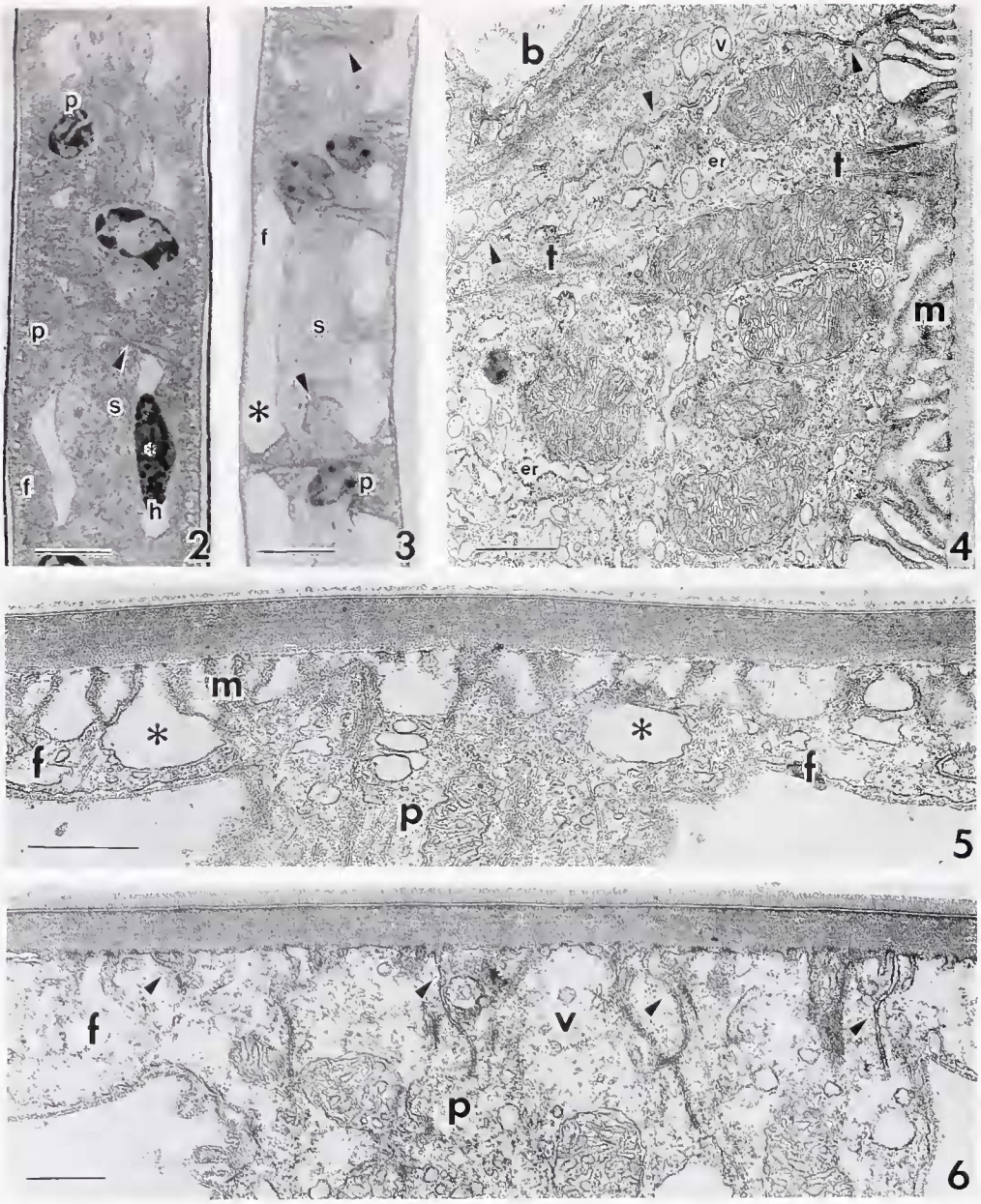

Figure 2. Thick (0.5 μm), epoxy section, taken transversely to the long axis of a gill lamella from *Macrobrachium olfersii* acclimated to fresh water (FW, < 0.5‰), showing the pillar cell perikarya (p) and thick flanges (f) below the subcuticular space. The intralamellar septum (s) adjoins the pillar cell perikarya (arrowhead). A hemocyte (*) is present in the hemolymph space (h). Scale bar = 10 μm.

Figure 3. Thick, epoxy section taken transversely to the long axis of a gill lamella from *M. olfersii* acclimated to seawater (SW) 28‰ for 10 days. The marked reduction in thickness of the pillar cell flanges (f) and septal cells (s) results in extensive hemolymph spaces (*). There is a distinct difference in cytoplasmic density (arrowheads) between the dark pillar (p) and light septal cells (s). Scale bar = 10 μm.

Figure 4. Transmission electron micrograph of a thin section taken transversely to the long axis of a gill lamella from *M. olfersii* in FW, showing the apical cytoplasm directly above the perikarya of two adjacent pillar cells, separated by a long, junctional complex (arrowheads). Apical microvilli (m), numerous vesicles (v), mitochondria, cisternae of rough endoplasmic reticulum (er), and microtubule bundles (t) are present. A basal lamina (b) separates the pillar cell membrane from the hemolymph space. Scale bar = 0.7 μm.

Figure 5. Electron micrograph of the apical region of a pillar cell perikaryon (p) and the bases of its lateral flanges (f) in a section taken transversely to the long axis of a gill lamella from *M. olfersii* acclimated to SW 21‰ for 10 days. The reduction in the height and numerical density of the apical microvilli (m) and in the thickness of the flanges is evident. The subcuticular space (*) between and below the microvilli is still present. Scale bar = 0.75 μm.

Morphometric measurements were made using a transparent test overlay consisting of parallel line segments each 1 cm in length, equally spaced at 1-cm intervals (Weibel *et al.*, 1966; Freire and McNamara, 1995). To measure the thickness of the septal cells, the test system was placed perpendicularly to the plane of the gill cuticle; valid transects were represented by single planes in which the line segments intersected both cell margins. To estimate the thickness of the pillar cell flanges, valid transects were single planes in which a line segment intersected at least one cell margin.

The heights of the apical microvilli were sampled both in the region above the pillar cell body and in the mid-flange region. The test system was placed parallel to the plane of the microvilli, and the heights of all microvilli intersecting one of the extremities of each line segment were measured. A height of 1 mm on the micrograph was considered to be the minimum length criterion representing a single microvillus.

The numerical density of the apical microvilli was also sampled in the same regions of the pillar cells. A second test system comprising a straight line 125 mm in length (equivalent to 5.0 μm at 25,000×) was placed over the micrograph at random, although parallel to the plane of the cuticle. All microvilli lying directly above the plane of the test line were counted.

All data were tested for normality of distribution using the Kolmogorov-Smirnov test. Non-normal data were normalized by transformation using the inverse function. Single- or two-factor analyses of variance were then performed to detect the effect of acclimation salinity on the various response variables. This was followed by multiple means testing, using the Student-Newman-Keuls test, when an effect was found. The data on microvillus height could not be normalized by transformation and were analyzed nonparametrically with the Friedman two-factor and Kruskal-Wallis one-factor analyses of variance. Differences between groups were located using the Wilcoxon-Mann-Whitney U test. All tests were performed using a minimum significance level of $P = 0.05$. The data are presented in the text as the mean ± 1 SEM (n) unless otherwise indicated.

Results

Figure 1, a diagram of the localization and general morphology of the gill lamella in *M. olfersii*, illustrates the organization of the gill tissue into a semiregular latticework of pillar and septal cells within the lamella. The present study focuses particularly on the ultrastructure of the flange and perikaryon regions of the pillar cells, which form the principal epithelial barrier between the hemolymph and the external medium.

Fine structure of the gill tissue in shrimps acclimated to fresh water

Pillar cells. The electron-dense pillar cells are highly differentiated epithelial cells constituted by two distinct regions: the pillar cell perikaryon, 7.8 ± 1.4 μm (n = 10) in height by 9.1 ± 5.8 μm (n = 14) in width (Fig. 2); and the pillar cell flange, a fine, roughly elliptical, radial, apical expansion of the perikaryon (Fig. 2), 56 ± 10 μm (n = 3) in diameter and 2.86 ± 0.16 μm (n = 6) in thickness near the perikaryon.

The apical membrane of the pillar cells, overlain by the fine gill cuticle [249.0 ± 4.4 nm (n = 10) thickness], is folded into an extensive system of microvilli (Fig. 4) that are organized into small tufts of from 4 to 8 villi (Fig. 7). These 10-nm diameter, cylindrical projections of the apical cytoplasm (Fig. 8) are frequently arranged into regularly spaced, often hexagonal, units and measure roughly 700 nm in height. The distribution and height of the microvilli are not uniform over the pillar cell surface: they are longer (Table I) and numerically more dense (Fig. 13) above the perikaryon (Fig. 4) than in the outer flange region (Fig. 9). A distinct subcuticular space, consisting mainly of the deeper invaginations between the tufts of microvilli (Figs. 2 and 7) and of large vesicles lying near the apical membrane (Fig. 9), is apparently continuous with these invaginations.

The electron-dense subapical cytoplasm immediately above the perikaryon (Fig. 4) contains numerous small vesicles; polyribosomes; mitochondria, frequently disposed with their long axes parallel to that of the perikaryon; cisternae of rough endoplasmic reticulum; and bundles of 23-nm diameter microtubules that insert into the base of each tuft of microvilli (Fig. 4). The nucleus occupies the basal region of the pillar cell perikaryon (Fig. 2), which is coupled to the adjacent cells of the intralamellar septum by regions of thick, basolateral junctions (Fig. 12). These junctions consist of a wide (109.3 ± 35.5 nm) intercellular space of variable form and length. The space, which contains granular material, leads to often complex, although limited, interdigitations between the plasmalemmae of the two cell types (Fig. 12, insert).

Figure 6. Electron micrograph of the apical region of a pillar cell perikaryon (p) and bases of its flanges (f) from *M. olfersii* acclimated to SW 28‰ for 10 days. The apical microvilli and subcuticular space have disappeared completely, being replaced by a few invaginations of the plasma membrane (arrowheads). Numerous vesicles (v) and mitochondria are present in the subapical cytoplasm. Scale bar = 0.4 μm.

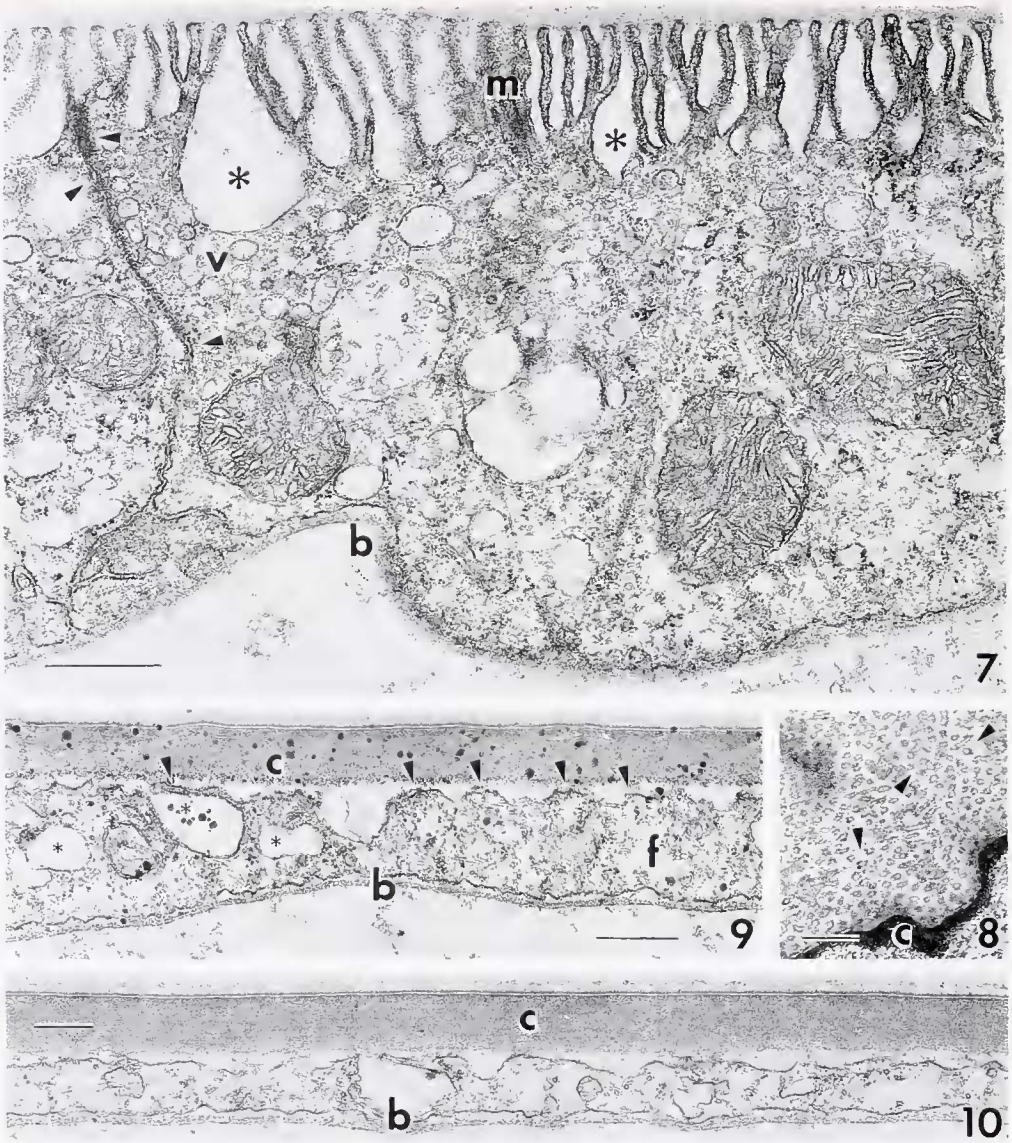

Figure 7. Transmission electron micrograph of a section taken transversely to the long axis of a gill lamella from *Macrobrachium olfersii* in FW, showing a region of the pillar cell flange, near the perikaryon, in junctional contact (arrowheads) with a flange from an adjacent pillar cell. Well developed, apical microvilli (m) are evident below the thin gill cuticle, as are numerous apical microvesicles (v), mitochondria, and the basal lamina (b) separating the uninvaginated, lower plasma membrane from the hemolymph. Subcuticular spaces (*) are present among and below the microvilli. Scale bar = 0.7 μm.

Figure 8. Thin section taken slightly obliquely to and just below the base of the gill cuticle (c) from *M olfersii* in FW, demonstrating that the apical infolding system is constituted by microvilli (arrowheads) rather than leaflets, seen here in transverse section. Scale bar = 0.7 μm.

Figure 9. Extreme, lateral region of a fine, pillar cell flange (f), distant from the perikaryon, underlain by basal lamina (b) from *M olfersii* in FW. The apical microvilli (arrowheads) have virtually disappeared below the cuticle (c), and only a few vesicles of the subcuticular space (*) and microtubules are present in the granular cytoplasm. Scale bar = 0.5 μm.

Figure 10. Extreme, lateral region of an apical, pillar cell flange, distant from the perikaryon, in the gill epithelium from *M olfersii* acclimated to SW 21‰ for 10 days. No apical microvilli are distinguishable below the cuticle (c), and only a very thin layer of cytoplasm containing a few microtubules is visible above the basal lamina (b) and underlying hemolymph space. Scale bar = 0.3 μm.

Table I

Effect of acclimation to saline media for 10 days on various morphometric characteristics analyzed in the gill lamellae of the freshwater shrimp Macrobrachium olfersii

Characteristic	Acclimation salinity (‰)		
	<0.5	21	28
Thickness of pillar cell flange (μm)	1.30 ± 0.20 (11)	[a]0.34 ± 0.04 (10)	[a]0.40 ± 0.05 (11)
Density of microvilli in pillar cell flange	[b]4.00 ± 0.50 (11)	[b]2.70 ± 0.40 (12)	[bcd]1.00 ± 0.40 (12)
Density of microvilli above pillar cell perikaryon	6.20 ± 0.40 (12)	5.00 ± 0.20 (12)	[c]4.00 ± 0.60 (12)
Thickness of septal cell (μm)	7.80 ± 0.50 (10)	7.10 ± 0.50 (10)	6.50 ± 0.60 (13)

Data are given as mean values ± SEM (n). Numerical densities are expressed as the number of microvilli per micrometer of linear apical membrane.

[a] $P \leq 0.05$ compared to control thickness in 0 ‰; [b] $P \leq 0.05$ compared to values for perikaryon; [c] $P \leq 0.05$ compared to value for flange in 0 ‰; [d] $P \leq 0.05$ compared to value for flange in 21 ‰; [e] $P \leq 0.05$ compared to value for perikaryon in 0 ‰.

The apical flange region of the pillar cells becomes attenuated and thinner as the distance from the perikaryon increases, attaining only 1.38 ± 0.30 μm (n = 6) in thickness at the extreme margins (Fig. 9). The number and height of the microvilli and organelles likewise decrease markedly; the mitochondria exhibit no specific orientation. Like the pillar cell perikaryon (Fig. 4), the entire lower surface of the pillar cell flange is underlain by a fibrous basal lamina (Figs. 7 and 9), thickness 92.8 ± 11.0 nm (n = 8), that separates it from the hemolymph space. The plasma membrane of this lower surface is not folded or amplified in any way.

The regions of contact between adjacent pillar cell flanges constitute highly structured junctional complexes (Figs. 7 and 11). These typically comprise a short, dense desmosome of 287.4 ± 30.2 nm (n = 6) length, followed by an extensive septate junction of about 1.5 μm in length, and a long region of simple apposition of the two cell membranes, separated by a constant narrow distance of 17.8 ± 1.7 nm (n = 10).

Intralamellar septal cells. The electron-lucent septal cells, 12.0 ± 0.7 μm (n = 10) in thickness (Figs. 2 and 3), make contact with the hemolymph over most of their surface, which is greatly amplified and is characterized by many invaginations of the plasmalemma; these penetrate deeply into and extensively throughout the septal cell cytoplasm and appear to individually envelop each of the numerous ovoid mitochondria present within the cytoplasm (Fig. 12). The membrane infoldings define an extracellular space of constant width (22.0 ± 0.7 nm, n = 10) and maintain contact with the hemolymph. Typically, a single septal cell connects the bases of two adjacent pillar cells, its lateral ends interdigitating in a restricted manner with their basolateral membranes (Fig. 12, insert). Golgi bodies and glycogen granules are frequently found in the septal cells.

Ultrastructural and morphometric alterations induced in the gill tissue of shrimps acclimated to saline media

Various ultrastructural alterations appear in the pillar cells of the gill lamellae of *M. olfersii* after acclimation to the two saline media (21‰ and 28‰) for 10 days. Qualitatively similar, these modifications comprise substantial reductions in the thickness of the pillar cell flanges (Figs. 3 and 10) and in the height and density of the apical microvilli, both in the region above the pillar cell perikarya (Figs. 5 and 6) and in the attenuated flange regions (Fig. 10). In 21‰ salinity, the microvilli lose their characteristic tuft-like arrangement (Fig. 5), and the associated microtubule bundles are less evident. In 28‰, the microvilli are virtually absent, and only a few invaginations of the apical membrane are evident (Fig. 6).

There is a more subtle reduction in the thickness of the intralamellar septal cells (Fig. 3, *cf.* Fig. 2), the structural organization of which is maintained. With the reduction in thickness of the pillar cell flanges, and to a lesser extent of the intralamellar septal cells, there is a corresponding, marked increase in the volume of the hemolymph lacunae (Fig. 3, *cf.* Fig. 2).

These qualitative ultrastructural alterations were quantified through morphometrical evaluation; the principal findings for normally distributed data are presented in Table I. Figure 13 presents the data on the height of the apical microvilli for which a normal distribution could not be obtained.

Discussion

In the gill epithelium of *Macrobrachium olfersii*, the apical surface of the pillar cells is highly amplified by an extensive system of microvilli (type 2, see Cioffi, 1984). This system is found principally above the perikaryon, becoming attenuated in the extreme lateral regions. The lower surface of the pillar cell flange is not invaginated or associated with mitochondria, and it does not appear to be involved in active transport and salt movement. This is in strong contrast to the epithelial cells of the gill in brachyurans (Gilles and Péqueux, 1985), penaeids (Couch, 1977; Foster and Howse, 1978), and amphipods (Kikuchi *et al.*, 1993; Kikuchi and Matsumasa, 1995; Shires *et al.*, 1994). In these crustaceans, Na^+/K^+-ATPases are typically associated with the basolateral infold-

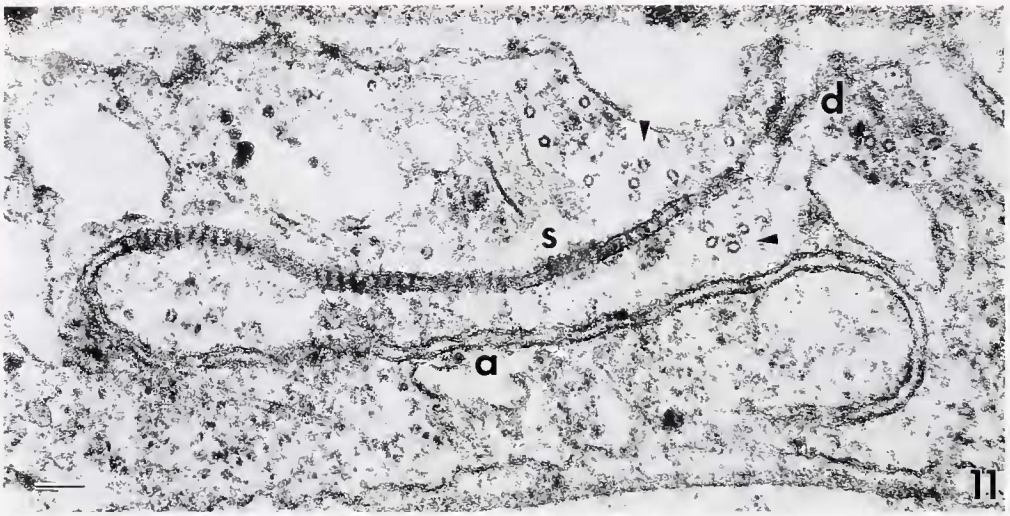

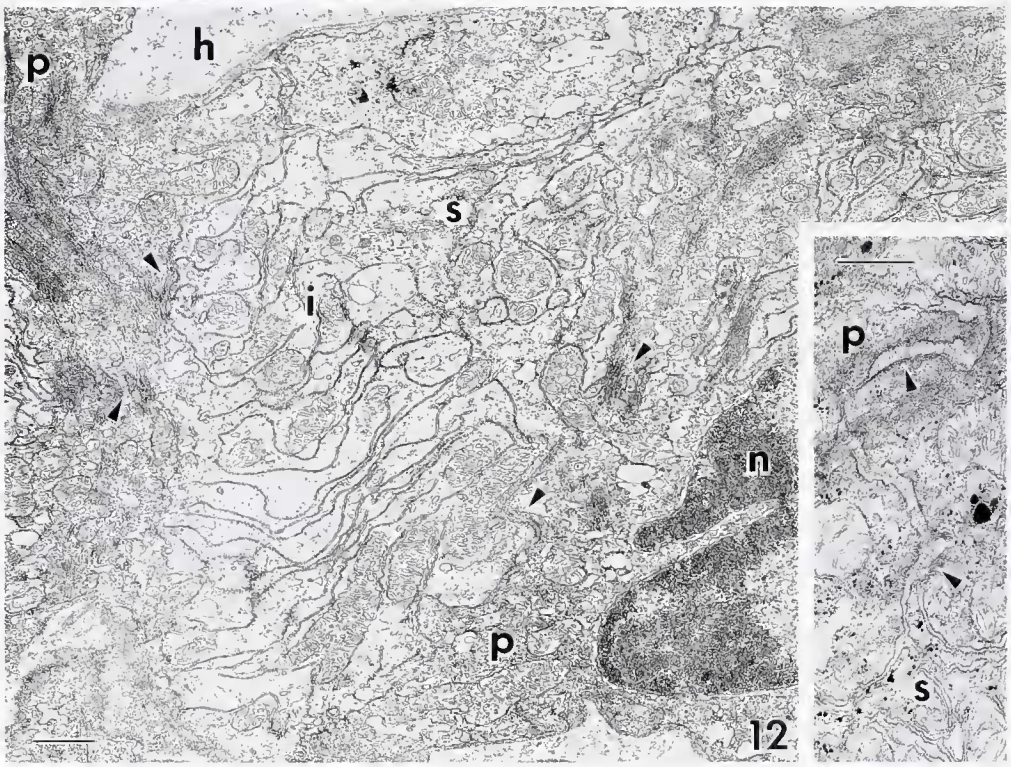

Figure 11. Detail of a characteristic junctional complex between the extreme, lateral flange regions of two adjacent pillar cells from *Macrobrachium olfersii* in FW. The sequence of a small desmosome (d), a shallow septate junction (s) and region of close membrane apposition (a) is typical. Small groups of microfilaments (arrowheads) are loosely associated with the apical region of the junction. Scale bar = 100 nm.

Figure 12. Transverse section of a gill lamella from *M. olfersii* in FW, showing a complex region of interdigitation between the bases of two electron dense, pillar cell perikarya (p) and an electron lucent cell in the interlamellar septum (s), characterized by extensive, deep invaginations (i) of the plasma membrane associated with mitochondria. Areas of dense, basolateral junctional complexes (arrowheads) link the two cell types. Pillar cell nucleus (n), hemolymph space (h). Scale bar = 1.0 μm. Insert: Detail of a thick, basolateral junction (arrowheads) between an interlamellar septal cell (s) and an abutting pillar cell (p), showing abundant finely granular material in the wide extracellular space. Scale bar = 0.5 μm.

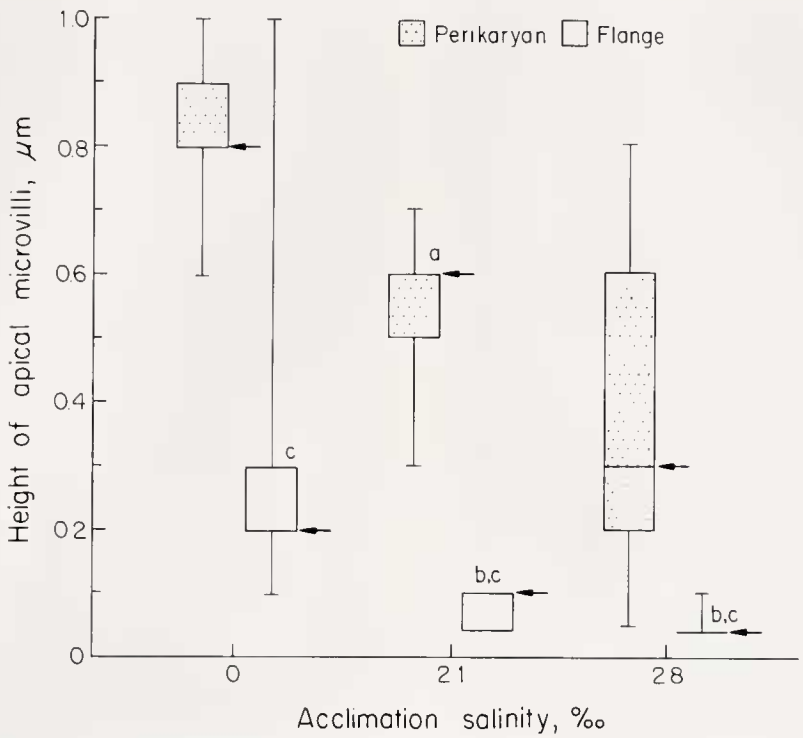

Figure 13. The effect of acclimation salinity (<0.5‰, 21‰, and 28‰) on the height of the apical microvilli in the region immediately above the pillar cell perikarya and in the extreme flange regions. The non-normally distributed data are given as the median values (arrows); the upper and lower box boundaries indicate the interquartile range; and the whiskers depict the minimum and maximum values. $^{a}P < 0.05$ compared to value for perikaryon in fresh water (< 0.5‰), $^{b}P < 0.05$ compared to value for flange in fresh water, $^{c}P < 0.05$ compared to respective values for perikarya in same salinities.

ings of the epithelial cells (see Towle, 1984; Towle and Kays, 1986; Taylor and Taylor, 1992) and actively drive salt uptake from the external medium directly into the hemolymph up a Na^+ gradient across the epithelium (see Péqueux, 1995, for review).

The differential distribution of the apical microvilli in *M. olfersii* attests to a dual role for the pillar cells in the regulatory physiology of the gill. The principal ion movements across the apical membrane occur through ion exchangers like the Na^+/NH_4^+ (Armstrong *et al.*, 1981) and Cl^-/HCO_3^- (Péqueux, 1995) counter transporters most likely present in the membranes of the long, dense microvilli located immediately above the pillar cell perikaryon, the region closest to the basolateral junctions with the septal cells. The exchange of respiratory gases, however, would be preferentially effected through the far less amplified surface of the shorter, less dense microvilli in the very thin, extreme flange regions that form a cytoplasmic barrier only 1.4 μm in thickness, directly above and in contact with the hemolymph space. This situation contrasts sharply with that known for brachyurans, in which respiratory gas-exchange functions predominate in the anterior gills, while ion transport mechanisms are more restricted to the posterior gills (Péqueux, 1995).

The notable reductions in the height and numerical density of the microvilli on the apical surface of the pillar cells, and in the thickness of the flanges, which occur as a result of acclimation to saline media in *M. olfersii*, are qualitatively similar to the modifications seen in the gill epithelia of a variety of osmoregulating crustaceans in response to exposure to either hyper- or hypo-osmotic media. In the brachyuran crabs *Eriochier sinensis* and *Carcinus maenas* acclimated to fresh water and 30% seawater, respectively, the apical infolding system becomes deeper and more pronounced, as does the subcuticular space (Gilles and Péqueux, 1985, 1986). In the latter crab, the depth of the basolateral invaginations and the number of mitochondria also appear to increase, with a closer degree of apposition between them (Compère *et al.*, 1989).

In the marine shrimp *Penaeus aztecus* exposed to a dilute medium of 0.9‰, the apical membranes of the epithelial cells become highly and deeply infolded compared to those of shrimps kept in seawater (Foster and

Howse, 1978). In this penaeid and *P. duorarum* (Couch, 1977) and *P. vannamei* (Taylor and Taylor, 1992, Fig. 25A), and in the palaemonid *Palaemonetes pugio* (Doughtie and Rao, 1978), the pillar cell perikarya appear to constitute part of the intralamellar septum. However, no changes seem evident in the septal cells of *P. aztecus* after low-salinity exposure (Foster and Howse, 1978). In *M. olfersii,* subtle changes in septal cell morphometry do occur after high-salinity acclimation: the number of membrane invaginations interposed between adjacent mitochondria increases, as does the surface density (square micrometers of membrane surface per cubic micrometer of cytoplasm) of the septal cells and the mitochondrial volume fraction; the mitochondrial profiles also become more elongate (Freire and McNamara, 1995).

In one of the few studies directly comparable to the present report (Shires *et al.,* 1994), a marked reduction occurred in the height and organization of the apical lamellae in the gill epithelial cells of the amphipod *Gammarus duebeni* within 1 h of exposure to seawater; the mitochondria relocated to the cell center and appeared to lose their intimate contact with both the apical and basolateral membrane systems. These alterations were transient, however, as the lamellae appeared to reorganize after 10–16 h.

These various data demonstrate the labile nature of the apical infoldings of the epithelial and pillar cells in the gill lamellae of osmoregulating crustaceans. The membrane surface area of this primary interface between the external medium and the hemolymph increases markedly during the acclimation of marine decapods to dilute media, and is notably decreased in freshwater Crustacea acclimated to saline media. This membrane system may thus serve primarily to modulate apical permeability by regulating the density of constituent ion-exchange molecules. In contrast, the system of basolateral infoldings and mitochondria in the epithelial cells of marine decapods appears largely unresponsive to decreased salinity; in freshwater Crustacea, exposure to saline media produces subtle alterations in membrane surface area and stacking, and in the location of the mitochondria.

The data on *M. olfersii,* both from shrimps maintained in fresh water (FW) and in those acclimated to saline media, also provide pertinent information about the routes of ion and water movements into the hemolymph through the gill tissue. In FW-acclimated shrimps, the gill epithelium appears to be a tight epithelium, well protected from paracellular water and ion movements by extensive and characteristic junctions—constituted by a small desmosome and a lengthy septate junction—between adjacent pillar cell flanges. These junctions are similar to those found in the gill epithelia of the freshwater amphipods *Sternomoera yezoensis* (Kikuchi *et al.,* 1993) and *Gammarus duebeni* (Shires *et al.,* 1994). The absence of mitochondria and infoldings of the basolateral membrane strongly suggests that the lower flange regions are not involved in active salt movement in *M. olfersii.*

However, the ultrastructure of the intralamellar septal cells, with their deep and numerous invaginations intimately associated with mitochondria, is typical of an active, salt-transporting epithelium in crustaceans and in a variety of invertebrate tissues (see Cioffi, 1984; Péqueux, 1995). Sites of Na^+/K^+-ATPase activity, demonstrated ultracytochemically, are present on the cytoplasmic surface of the leaflets of this extensive membrane system in *M. olfersii* (Torres and McNamara, 1996); their activity would be fueled by ATP furnished directly by the abundant adjacent mitochondria. In FW-acclimated shrimps, the activity of the Na^+/K^+-ATPases in the membrane invaginations of the septal cells creates the driving force for net Na^+ uptake from the freshwater medium across the apical membranes of the pillar cells into the perikarya. Na^+ would then pass through the extensive intercellular junctions between the base of the pillar cell perikarya and the lateral ends of the intralamellar septal cells into the septal cell cytoplasm, and from there directly into the hemolymph *via* the Na^+/K^+-ATPases in the membrane invaginations. Corroborating this proposed route of ion movement, Lima *et al.* (1997) have shown a significant reduction in Na^+/K^+-ATPase activity in preparations of gill membrane vesicles from *M. olfersii* after acclimation to saline media (21 and 28‰ salinity) for 20 days. This observation suggests a reduction in the number of ATPase molecules in these membranes available for active Na^+ transport.

The alterations occurring at the apical pillar cell interface, and other changes in the characteristics of the intralamellar septal cells, including the reduction in Na^+/K^+-ATPase activity, thus appear to reflect the structural transformations underlying the molecular mechanisms of long-term adaptation to hyperionic media in freshwater palaemonids, particularly those that restrict the uptake of Na^+.

Acknowledgments

This study represents part of an MSc thesis submitted by AGL to the Departamento de Fisiologia/IBUSP; it was financed by a research grant to JCM (FAPESP 91/2467-2) and a post-graduate scholarship (FAPESP 90/3807-9). The authors thank Drs. João Lunetta (CEBIMAR), Sergio Oliveira (DHE/ICB), and Valder de Melo (DM/FMRP) for access to essential facilities; José Augusto Maulin (DM/FMRP) for photographic work; and Marcos Ribeiro de Souza (FFCLRP) for the line drawing.

Literature Cited

Armstrong, D. A., K. Strange, J. Crowe, A. Knight, and M. Simmons. 1981. High salinity acclimation by the prawn *Macrobrachium rosenbergii*: uptake of exogenous ammonia and changes in endogenous nitrogen compounds. *Biol. Bull.* **160:** 349–365.

Barra, J.-A., A. Péqueux, and W. Humbert. 1983. A morphological study on gills of a crab acclimated to fresh water. *Tissue Cell* **15:** 583–596.

Bubel, A. 1976. Histological and electron microscopical observations on the effects of different salinities and heavy metal ions on the gills of *Jaera nordmanni* (Rathke) (Crustacea, Isopoda). *Cell Tiss. Res.* **167:** 65–95.

Cioffi, M. 1984. Comparative ultrastructure of arthropod transporting epithelia. *Am. Zool.* **24:** 139–156.

Compère, Ph., S. Wanson, A. Péqueux, R. Gilles, and G. Goffinet. 1989. Ultrastructural changes in the gill epithelium of the green crab *Carcinus maenas* in relation to external salinity. *Tissue Cell* **21:** 299–318.

Copeland, D. E. 1968. Fine structure of salt and water uptake in the land crab *Gecarcinus lateralis*. *Am. Zool.* **8:** 417–432.

Copeland, D. E., and A. T. Fitzjarrell. 1968. The salt absorbing cells in the gills of the blue crab (*Callinectes sapidus* Rathbun) with notes on modified mitochondria. *Z. Zellforsch.* **92:** 1–22.

Couch, J. A. 1977. Ultrastructural study of lesions in gills of a marine shrimp exposed to cadmium. *J. Invertebr. Pathol.* **29:** 267–288.

Doughtie, D. G., and K. R. Rao. 1978. Ultrastructural changes induced by sodium pentachlorophenate in the grass shrimp, *Palemonetes pugio*, in relation to the molt cycle. Pp. 213–250 in *Pentachlorophenol: Chemistry, Pharmacology, and Environmental Toxicology*, Vol. 12, K. R. Rao, ed. Plenum Press, New York.

Foster, C. A., and H. D. Howse. 1978. A morphological study on gills of the brown shrimp, *Penaeus aztecus*. *Tissue Cell* **10:** 77–92.

Freire, C. A., and J. C. McNamara. 1995. Fine structure of the gills of the fresh-water shrimp *Macrobrachium olfersii* (Decapoda): effect of acclimation to high salinity medium and evidence for involvement of the intralamellar septum in ion uptake. *J. Crustac. Biol.* **15:** 103–116.

Gilles, R., and A. Péqueux. 1985. Ion transport in crustacean gills: physiological and ultrastructural approaches. Pp. 136–158 in *Transport Processes, Iono- and Osmoregulation*, R. Gilles and M. Gilles-Biallien, eds. Springer-Verlag, Berlin.

Gilles, R., and A. Péqueux. 1986. Physiological and ultrastructural studies of NaCl transport in crustacean gills. *Bol. Zool.* **53:** 173–182.

Kikuchi, S., M. Matsumasa, and Y. Yashima. 1993. The ultrastructure of the sternal gills forming a striking contrast with the coxal gills in a fresh-water amphipod (Crustacea). *Tissue Cell* **25:** 915–928.

Kikuchi, S., and M. Matsumasa. 1995. Pereopodal disk: a new type of extrabranchial ion-transporting organ in an estuarine amphipod, *Melita setiflagela* (Crustacea). *Tissue Cell* **27:** 635–643.

Lima, A. G., J. C. McNamara, and W. R. Terra. 1997. Regulation of hemolymph osmolytes and gill Na^+/K^+-ATPase activities during acclimation to saline media in the freshwater shrimp *Macrobrachium olfersii* (Wiegmann, 1836) (Decapoda, Palaemonidae). *J. Exp. Mar. Biol. Ecol.* In press.

Maina, J. N. 1990. The morphology of the gills of the freshwater African crab *Potamon niloticus* (Crustacea: Brachyura: Potamonidae): a scanning and transmission electron microscopic study. *J. Zool.* **221:** 499–515.

Mantel, L. H., and L. L. Farmer. 1983. Osmotic and ionic regulation. Pp. 53–161 in *The Biology of Crustacea*, Vol. 5, *Internal Anatomy and Physiological Regulation*, L. H. Mantel, ed. Academic Press, New York.

McNamara, J. C. 1987. The time course of osmotic regulation in the freshwater shrimp *Macrobrachium olfersii* (Wiegmann) (Decapoda, Palaemonidae). *J. Exp. Mar. Biol. Ecol.* **107:** 245–251.

Nakao, T. 1974. Electron microscopic study of the open circulatory system of the shrimp, *Caridina japonica* 1. Gill capillaries. *J. Morphol.* **144:** 361–380.

Péqueux, A. 1995. Osmotic regulation in crustaceans. *J. Crustac. Biol.* **15:** 1–60.

Reynolds, E. S. 1963. The use of lead citrate at high pH as an electron-opaque stain in electron microscopy. *J. Cell Biol.* **17:** 208–212.

Shires, R., N. J. Lane, C. B. Inman, and A. P. Lockwood. 1994. Structural changes in the gill cells of *Gammarus duebeni* (Crustacea, Amphipoda) under osmotic stress; with notes on microtubules in association with the septate junctions. *Tissue Cell* **26:** 767–778.

Taylor, H. H., and E. W. Taylor. 1986. Observations of valve-like structures and evidence for rectification of flow within the gill lamellae of the crab *Carcinus maenas* (Crustacea, Decapoda). *Zoomorphology* **106:** 1–11.

Taylor, H. H., and E. W. Taylor. 1992. Gills and lungs: the exchange of gases and ions. Pp. 203–293 in *Microscopic Anatomy of Invertebrates*, Vol. 10, *Decapod Crustacea*, F. W. Harrison and A. G. Humes, eds. Wiley-Liss, Inc., New York.

Torres, A. H., and J. C. McNamara, 1996. Localização ultracitoquímica da ATPase Na^+/K^+-dependente em células de brânquia e glândula antenal do camarão de água doce *Macrobrachium olfersii*. IV Simpósio de Iniciação Científica da Universidade de São Paulo, Abstracts, p. 132.

Towle, D. W. 1984. Membrane-bound ATPases in arthropod ion-transporting tissues. *Am. Zool.* **24:** 177–185.

Towle, D. W., and W. T. Kays. 1986. Basolateral localization of $Na^+ + K^+$-ATPase in gill epithelium of two osmoregulating crabs, *Callinectes sapidus* and *Carcinus maenas*. *J. Exp. Zool.* **239:** 311–318.

Weibel, E. R., G. S. Kistler, and W. F. Scherle. 1966. Practical stereological methods for morphometric cytology. *J. Cell Biol.* **30:** 23–28.